Photoinduced Charge Separation and Recombination in a Novel Methanofullerene−Triarylamine Dyad Molecule

Satoshi Komamine,[†] Mamoru Fujitsuka,[†] Osamu Ito,*[,†] Kazuyuki Moriwaki,[‡] Toshiyuki Miyata,[‡] and Toshinobu Ohno*[,‡]

Institute for Chemical Reaction Science, Tohoku University, Katahira, Aoba-ku, Sendai 980-8577, Japan, and Osaka Municipal Technical Research Institute, Morinomiya, Joto-ku, Osaka 536-8553, Japan

Received: June 30, 2000; In Final Form: September 8, 2000

Intramolecular charge separation (CS) and charge recombination (CR) processes of the dyad molecule linking C_{60} and *N*,*N*-di(6-*tert*-butylbiphenyl)benzenamine (BBA) were investigated by pico- and nanosecond laser flash photolysis methods. Furthermore, intermolecular electron transfer to a methanofullerene ($C_{61}H_2$) was also investigated; the electron-transfer rate between triplet excited $C_{61}H_2$ and BBA was somewhat slower than that of C_{60} due to less negative reduction potential of $C_{61}H_2$. As for the BBA−C_{60} dyad molecule, CS was successfully observed in polar solvents by excitation of C_{60} moiety with picosecond laser pulse, while only the intersystem crossing was observed in nonpolar solvent. The CS process in the Marcus "normal region" was confirmed. In moderately polar solvent, radical ion pairs recombined within a few nanoseconds to generate the ground state and the triplet excited state of the C_{60}-moiety. On the other hand, in polar solvents, the radical ion pairs decayed by two-steps: Most part decayed within 1 ns, while the radical ions were also observed in the submicrosecond region for a ca. 10% yield of generated BBA$^{\bullet+}$-$C_{60}^{\bullet-}$. An equilibrium between CS and triplet states was proposed for the mechanism of long-lived CS state.

Introduction

Fullerene C_{60} and its derivatives exhibit a number of distinctive electronic and photophysical properties, which have been investigated for application to novel molecular electronic devices. Since fullerenes are good electron acceptors in the excited states, several photoinduced functions are expected for the materials composed of fullerene and electron donors. To achieve highly efficient charge separation (CS) between donor and acceptor, linking them with covalent bonds is an important and powerful strategy.[1] Recently, functionalizations of fullerenes with donor molecules have been attempted by several groups.[2−8] As for donors of the dyad molecules, aromatic amino compounds,[3] carotenoid,[4] porphyrin,[4] tetrathiafulvalene,[5] oligothiophene,[7] and so on[8] have been employed. These fullerene-donor linked molecules on the electrode exhibit excellent photovoltaic effects upon photoirradiation.[5d,7d] These interesting properties can be attributed to high efficiency of CS in the fullerene-donor linked molecules.

Among the several donor molecules, triarylamines are known to form stable radical cations and are often employed for the building blocks for electron and hole-transport layer in electroluminescent devices,[9] which indicates that utilization of triarylamines in the dyad molecule is beneficial for the materialization. Therefore, triarylamines are important candidates for the donor moieties of the fullerene-donor linked molecules. Furthermore, their characteristic and intense absorption bands of radical ions are very useful for the investigation of the CS and charge recombination (CR) dynamics of the dyad molecules. From these reasons, *N*,*N*-di(6-*tert*-butylbiphenyl)-benzenamine (BBA, Figure 1) was employed as a donor moiety of the dyad in the present paper. As for the fullerene moiety, methanofullerene was employed. Photophysics of methanofullerenes have been reported by some researchers.[10]

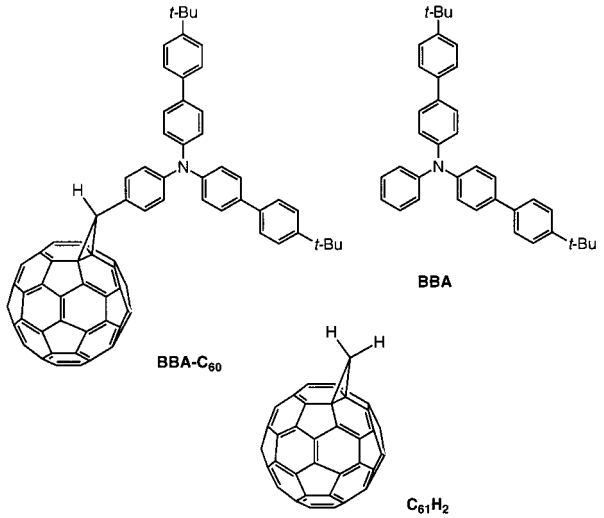

Figure 1. Molecular Structures of $C_{61}H_2$, BBA, and BBA−C_{60}.

In the first part of the present paper, we investigated the intermolecular electron-transfer processes between BBA and methanofullerene ($C_{61}H_2$) in polar solvents, because these data are indispensable for the study of the photoinduced CS and CR processes of the dyad molecule. Then, photoinduced CS and CR processes of BBA−C_{60} dyad molecule, which was linked by three σ-bonds, were characterized on the basis of the results of pico- and nanosecond laser flash photolysis. Furthermore, CR processes were found to depend on the solvent polarity to a great extent.

* Authors to whom correspondence should be addressed.
[†] Tohoku University.
[‡] Osaka Municipal Technical Research Institute.

10.1021/jp002319b CCC: $19.00
Published on Web 11/17/2000

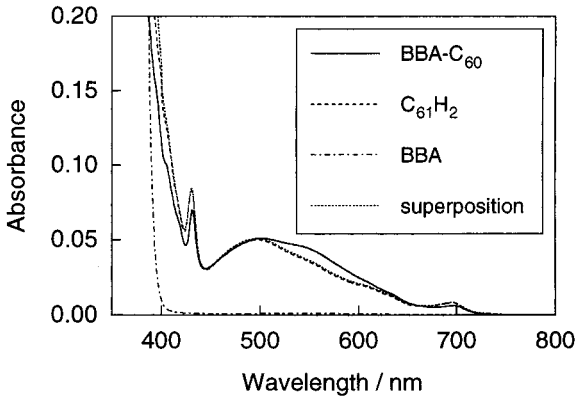

Figure 2. Steady-state absorption spectra of $C_{61}H_2$, BBA, and BBA−C_{60} in toluene. Superposition indicates linear combination of spectra of $C_{61}H_2$ and BBA.

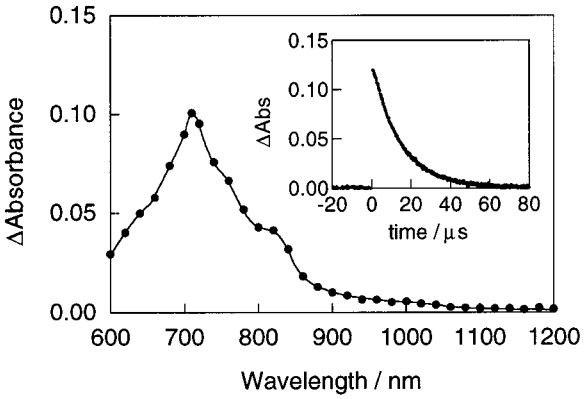

Figure 3. Transient absorption spectrum of $C_{61}H_2$ in toluene at 5 μs after 532 nm laser excitation. Inset: Absorption−time profile at 710 nm.

Experiments

Syntheses of BBA−C_{60} and $C_{61}H_2$ are described elsewhere.[11] Other chemicals were of the best grade commercially available. Steady-state absorption spectra were measured on a JASCO V-530 UV/VIS spectrophotometer. Steady-state fluorescence spectra were measured on a Shimadzu RF-5300 PC spectrofluorophotometer.

Fluorescence lifetimes were measured by a single-photon counting method using a second harmonic generation (SHG, 410 nm) of a Ti:sapphire laser (Spectra-Physics, Tsunami 3950-L2S, fwhm 1.5 ps) with a streak scope (Hamamatsu Photonics, C4334−01).

Nanosecond transient absorption spectra were measured using SHG (532 nm) of a Nd:YAG laser (Spectra-Physics, Quanta-Ray, GCR-130, fwhm 6 ns) as an excitation source. For measurements in the near-IR and visible regions, a Ge avalanche photodiode (Hamamatsu Photonics, B2834) was used as a detector for monitoring light from a pulsed Xe-lamp. In the visible region, Si-PIN photodiode (Hamamatsu Photonics, S1722-02) was used as a detector. The sample solutions contained in a 10 mm quartz cell were deaerated with Ar bubbling before measurements at ambient temperature.

The picosecond laser flash photolysis was carried out using SHG (532 nm) of an active/passive mode-locked Nd:YAG laser (Continuum, PY61C-10, fwhm 35 ps) as the excitation light. A white continuum light generated by focusing the fundamental of the Nd:YAG laser on a D_2O/H_2O (1:1 volume) cell was used as the monitoring light. The monitoring light transmitted through the sample was detected with a dual MOS detector (Hamamatsu Photonics, C6140) equipped with a polychromator.[7b]

Cyclic volumetric measurements were carried out with a potentiostat (Hokuto Denko, HAB-151) and a cell equipped with a platinum working electrode, an Ag/AgCl reference electrode, and platinum counter electrode at scan rates of 100 mV s^{-1}. All electrochemical measurements were performed in benzonitrile solution containing 0.10 M of *tetra-n*-butylammonium hexafluorophosphate (Nacalai Tesque) at room temperatures.

Results and Discussion

Steady-State Spectra. Steady-state absorption spectra of BBA−C_{60}, $C_{61}H_2$, and BBA in toluene are shown in Figure 2. The absorption spectrum of BBA−C_{60} is similar to the superposition of the spectra of BBA and C_{60}, although slight deviation was observed around 500−600 nm region. This finding indicates weak electronic interaction between the donor and fullerene moieties in the ground state due to quite close distance between the chromophores, which are bridged by three σ-bonds. The weak electronic interaction is in accord with the fact that the first reduction and oxidation potentials of BBA−C_{60} were estimated to be −0.42 and +1.02 V vs Ag/AgCl, respectively, which are shifted to anodic potentials compared with the redox potentials of the components; the reduction potential of $C_{61}H_2$ and the oxidation potential of BBA were −0.54 and +0.95 V, respectively.

In the present study, laser excitation of BBA−C_{60} was conducted at either 532 or 410 nm. Since BBA does not show substantial absorbance at both wavelengths, excited states of fullerene moiety play an important roll in the photoinduced processes, such as CS and CR. As for the mixture system of $C_{61}H_2$ and BBA, photoinduced processes are also expected to proceed via the excited $C_{61}H_2$ for the same reason.

Excited Properties of $C_{61}H_2$. At first, excited properties of $C_{61}H_2$ were investigated, since $C_{61}H_2$ is the component of the BBA−C_{60} dyad molecule. The transient absorption spectrum of $C_{61}H_2$ in toluene was shown in Figure 3. A sharp absorption band appeared at 710 nm immediately after the laser irradiation, which decays within a hundred microseconds in toluene. The transient absorption band at 710 nm was quenched in the presence of triplet state quenchers such as oxygen and β-carotene. These results suggest that this absorption peak is due to the excited triplet state of $C_{61}H_2$($^3C_{61}H_2$*). The spectral shape is similar to the triplet−triplet absorption spectrum of C_{60}, but the peak shifted ~40 nm to shorter wavelength side. Its triplet−triplet extinction coefficient at 710 nm was evaluated to be 12000 M^{-1} cm^{-1} from the energy transfer to β-carotene. Furthermore, it was confirmed that $^3C_{61}H_2$* decayed by the triplet−triplet annihilation and the self-quenching processes, the bimolecular rate constants were estimated to be 1.3×10^9 and 1.2×10^9 M^{-1} s^{-1}, respectively.

Upon excitation at 410 nm, $C_{61}H_2$ showed a fluorescence band at 705 nm, indicating the lowest excited singlet energy is 1.76 eV. Furthermore, the fluorescence lifetime and quantum yield were evaluated to be 1.4 ns and 5.6×10^{-4}, respectively, which were similar values to those of C_{60}.[12−14]

Photoinduced Electron Transfer of $C_{61}H_2$ and BBA Mixture System. In the presence of BBA in benzonitrile, upon excitation of $C_{61}H_2$, new transient absorption bands appeared at 380 and 910 nm (Figure 4), which are attributed to $BBA^{\bullet+}$ (See Supporting Information, Figure 1S). Since $BBA^{\bullet+}$ was generated with the decay of $^3C_{61}H_2$* at 710 nm, the electron transfer proceeded from BBA to $^3C_{61}H_2$* (eq 1):

$$^3C_{61}H_2^* + BBA \xrightarrow{k_{et}} C_{61}H_2^{\bullet-} + BBA^{\bullet+} \qquad (1)$$

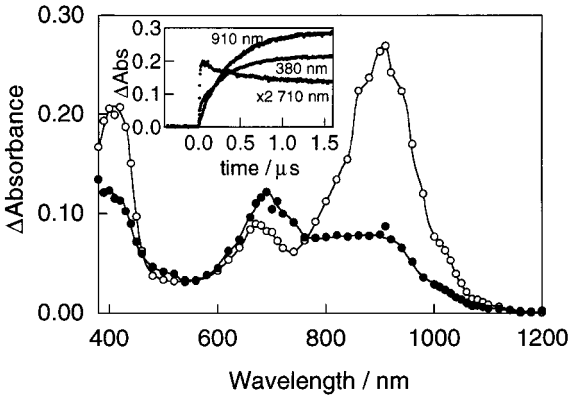

Figure 4. Transient absorption spectra of $C_{61}H_2$ (1.0×10^{-4} M) in the presence of BBA (4.0×10^{-3} M) in benzonitrile at 100 ns (closed circle) and 1 μs (open circle) after 532 nm laser excitation. Inset: Absorption−time profiles at 910, 710, and 380 nm.

From the chemical reduction of $C_{61}H_2$ by tetrakis(dimethylamino)ethylene,[15] it was revealed that $C_{61}H_2^{\bullet-}$ shows an absorption band at 1035 nm. In Figure 4, the absorption band due to $C_{61}H_2^{\bullet-}$seems to be hidden by the absorption band of $BBA^{\bullet+}$, indicating a larger extinction coefficient of $BBA^{\bullet+}$.

The rise rate of $BBA^{\bullet+}$ at 910 nm increased with an increase in concentration of BBA in the mixture system. From the pseudo first-order plot, triplet quenching rate constant (k_q^T) was estimated to be 6.5×10^8 M^{-1} s^{-1}. The k_q^T value was smaller than that observed for the reaction between $^3C_{60}$* and BBA ($k_q^T = 2.8 \times 10^9$ M^{-1} s^{-1}) by a factor of 1/4. The smaller k_q^T value of $C_{61}H_2$ is in accord with the prediction based on the free-energy changes for the electron-transfer processes (ΔG_{et}).[16] The ΔG_{et} values were calculated to be −0.23 and −0.41 eV for electron transfer via $^3C_{61}H_2$* and $^3C_{60}$*, respectively, from the redox potentials and the lowest triplet energies ($^3E_{00} = 1.50$ and 1.56 eV for $^3C_{61}H_2$* and $^3C_{60}$*, respectively).[17]

In the mixture system of $C_{61}H_2$ and BBA, the absorption band of $^3C_{61}H_2$* was quenched in the presence of oxygen (Figure 5 a), on the other hand, the decay rate of $BBA^{\bullet+}$ was not accelerated by oxygen as indicated in Figure 5B, while generation yield of $BBA^{\bullet+}$ decreased due to quenching of $^3C_{61}H_2$*, which is the precursor of the electron-transfer process. Furthermore, we recently reported that the reaction rate between the radical anion of pristine C_{60} and oxygen is as slow as 3.7×10^2 M^{-1} s^{-1}.[18] These facts indicate that scavenge of radical ions by oxygen is not a fast reaction after completion of electron transfer.

The absorption intensity of $BBA^{\bullet+}$ at 910 nm decayed slowly after the formation of the radical ion. This decay obeyed the second-order kinetics and is attributed to the back electron-transfer process (eq 2):

$$C_{61}H_2^{\bullet-} + BBA^{\bullet+} \xrightarrow{k_{bet}} C_{61}H_2 + BBA \qquad (2)$$

From the slope of the second-order plot yielding k_{bet}/ϵ_C ($= 5.0 \times 10^5$ cm s^{-1}, where k_{bet} and ϵ_C are a rate constant for the back electron transfer and an extinction coefficient of the radical cation, respectively), k_{bet} was evaluated to be 2.0×10^{10} M^{-1} s^{-1} using ϵ_C value of $BBA^{\bullet+}$ (4.0×10^4 M^{-1} cm^{-1}).[19] The k_{bet} value for $C_{61}H_2^{\bullet-}$ and $BBA^{\bullet+}$ was almost the same as that of $C_{60}^{\bullet-}$ and $BBA^{\bullet+}$ (1.7×10^{10} M^{-1} s^{-1}), indicating that the both back electron transfers are the diffusion-limiting processes due to sufficiently negative free-energy changes.

Fluorescence Spectra of BBA−C_{60} Dyad. Figure 6 shows the fluorescence spectrum of BBA−C_{60} in toluene by excitation

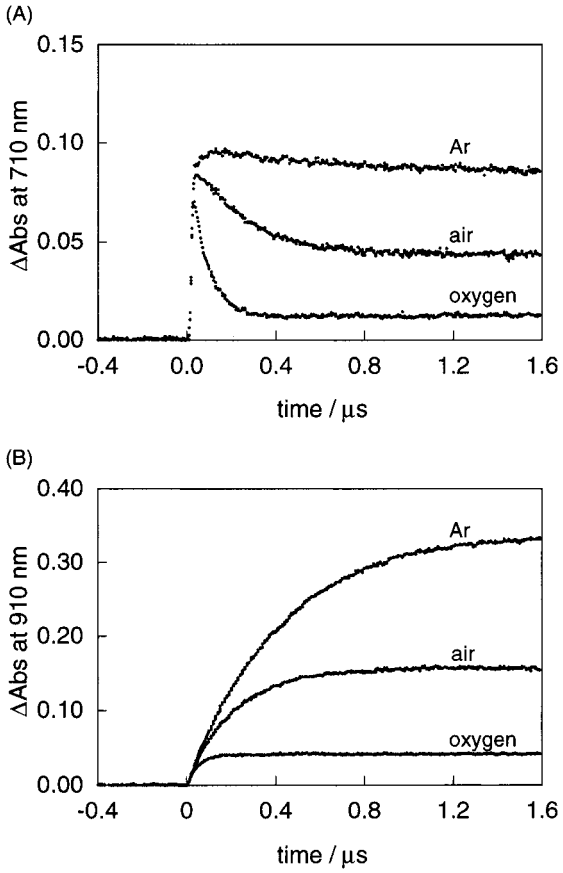

Figure 5. Absorption−time profiles (A) at 710 nm and (B) at 910 nm of $C_{61}H_2$ in the presence of BBA (4.0×10^{-3} M) in argon-, air-, and oxygen-saturated benzonitrile solution.

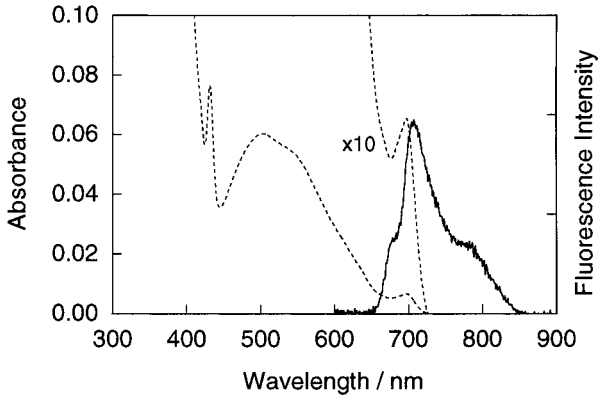

Figure 6. Fluorescence (solid line) and absorption (broken line) spectra of BBA−C_{60} in toluene.

at 410 nm. The fluorescence spectrum was a mirror image of the absorption spectrum around 700 nm as in the case of $C_{61}H_2$, indicating that this fluorescence spectrum is originated from the fullerene moiety. The BBA−C_{60} showed small Stokes shift, and the lowest singlet excited energy ($^1E_{00}$) was evaluated to be 1.76 eV. In more polar solvents, however, no fluorescence was observed from the C_{60} moiety of the BBA−C_{60} dyad. Thus, a new quenching pathway takes part in the deactivation processes of BBA−$^1C_{60}$* in these polar solvents.

Fluorescence decay profiles of BBA−C_{60} in toluene and anisole were obtained by a single-photon counting method as represented in Figure 7. The fluorescence decay in nonpolar toluene was fitted with a single-exponential function and gave a lifetime of 1.4 ns (Figure 7 A), which is the same as that of $C_{61}H_2$ (1.4 ns). In more polar anisole, fluorescence decay was

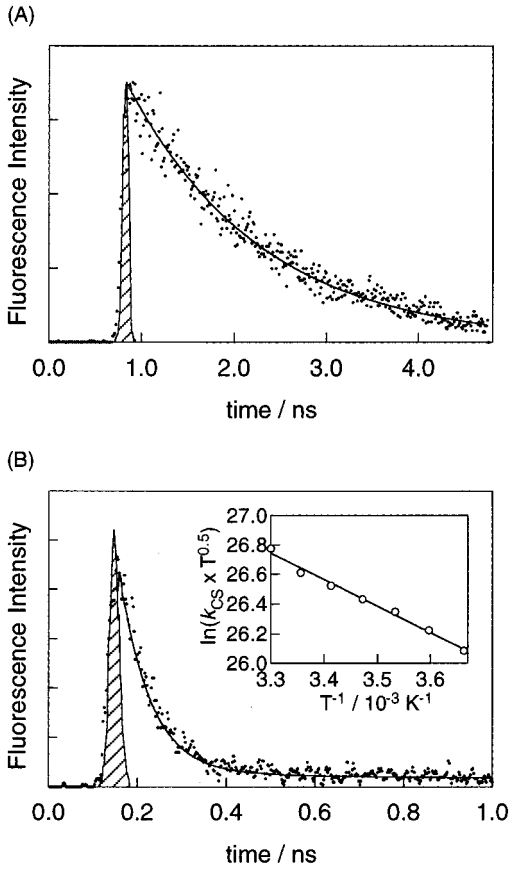

Figure 7. Fluorescence decays of BBA−C_{60} at 710 nm (A) in toluene and (B) in anisole. Fitted curves and laser profiles are also shown by solid lines and hatched curves, respectively. Inset: Modified Arrhenius plot $\ln(k_{CS} \times T^{0.5}) = \ln(k_{opt}) - (\Delta G^{\#}_{CS}/k_B) \times 1/T$ for BBA−C_{60} in anisole.

substantially accelerated (Figure 7B). Although the fluorescence decay needs two exponential functions for adequate fit, the slow decay-component (ca. 1.0 ns of lifetime) is a quite minor contribution (<5%). The slow decay component will be due to the decomposed compounds, because the contribution of the slow component increased for repeatedly laser-irradiated sample. On the other hand, the lifetime of the fast decay component was 50 ps. The fluorescence lifetime of BBA−C_{60} was evaluated in a variety of solvents (Table 1). It should be noted that the fluorescence lifetime of BBA−C_{60} became shorter as the polarity of the solvent became higher. Therefore, CS in BBA−C_{60} is a possible deactivation process in the polar solvents. Furthermore, the fluorescence lifetime of BBA−C_{60} showed temperature dependence as discussed in the latter section.

Picosecond Transient Absorption Spectra of BBA−C_{60} Dyad. The photoinduced processes of BBA−C_{60} were investigated in detail by picosecond transient absorption spectra using the 532 nm laser pulse. Figure 8 A shows transient absorption spectra of BBA−C_{60} in toluene. At 250 ps after the laser excitation, a transient absorption band with a peak around 900 nm was confirmed, which was assigned to the singlet excited state of the C_{60} moiety (BBA−$^1C_{60}$*).[10b] The decay lifetime of BBA−$^1C_{60}$* at 900 nm was estimated to be 1.2 ns (Figure 8 B), which is close to the fluorescence lifetimes of BBA−C_{60} and $C_{61}H_2$ in toluene. At 2.7 ns, another absorption band appeared around 700 nm, which can be attributed to the triplet excited state of the C_{60} moiety (BBA−$^3C_{60}$*) from the comparison with the absorption spectrum of $^3C_{61}H_2$* (Figure 3).[10a,e,g] The absorption−time profile at 700 nm dose not show absorbance change in the estimated time region (Figure 8B), because of the overlap

TABLE 1: Free-Energy Changes for CS (ΔG_{CS}), Fluorescence Lifetimes (τ_F), CS Rates (k_{CS}), and Quantum Yields for CS of BBA−C_{60} (Φ_{CS}) in Various Solvents

solvent[a]	ϵ_S	$-\Delta G_{CS}$/eV[b]	τ_F/s	k_{CS}/s^{-1} [c]	Φ_{CS}[d]
BN	25.2	0.39	2.0×10^{-11}	5.0×10^{10}	0.98
ANS/BN	14.8	0.33	2.6×10^{-11}	3.8×10^{10}	0.98
THF	7.58	0.27	2.9×10^{-11}	3.4×10^{10}	0.98
ANS	4.33	0.12	5.0×10^{-11}	1.9×10^{10}	0.95
ANS/Tol	3.36	0.03	6.7×10^{-11}	1.4×10^{10}	0.95
Tol	2.38	−0.15	1.4×10^{-9}		0.00

[a] BN, benzonitrile; ANS/BN, anisole/benzonitrile (1:1) mixture; THF, tetrahydrofuran; ANS, anisole; ANS/Tol, anisole/toluene (1:1) mixture; Tol, toluene. [b] $\Delta G_{CS} = E_{ox}(D) - E_{red}(A) - {}^1E_{00} + \Delta G_S$, $\Delta G_S = e^2/(4\pi\epsilon_0)[(1/(2r^+) + 1/(2r^-) - 1/R_{cc})(1/\epsilon_s) - (1/(2r^+) + 1/(2r^-))(1/\epsilon_r)]$, where $E_{ox}(D)$ and $E_{red}(A)$ are donor and acceptor redox potentials (+1.02 V and −0.42 V vs Ag/AgCl) and ${}^1E_{00}$ is the singlet excited energy of the fullerene moiety (${}^1E_{00}$ = 1.76 eV). The ϵ_s and e_r are static dielectric constants of solvents used for the rate measurements and the redox-potential measurements. R_{cc} is the center-to-center distance (12.4 Å) and r^+ and r^- are the effective ionic radii of the donor (7.4 Å) and acceptor (4.9 Å), respectively. [c] $k_{CS} = 1/\tau_F - 1/\tau_{ref}$, where τ_{ref} is fluorescence lifetime of $C_{61}H_2$ in toluene. [d] $\Phi_{CS} = ((\tau_F)^{-1} - (\tau_{ref})^{-1})/(\tau_F)^{-1}$.

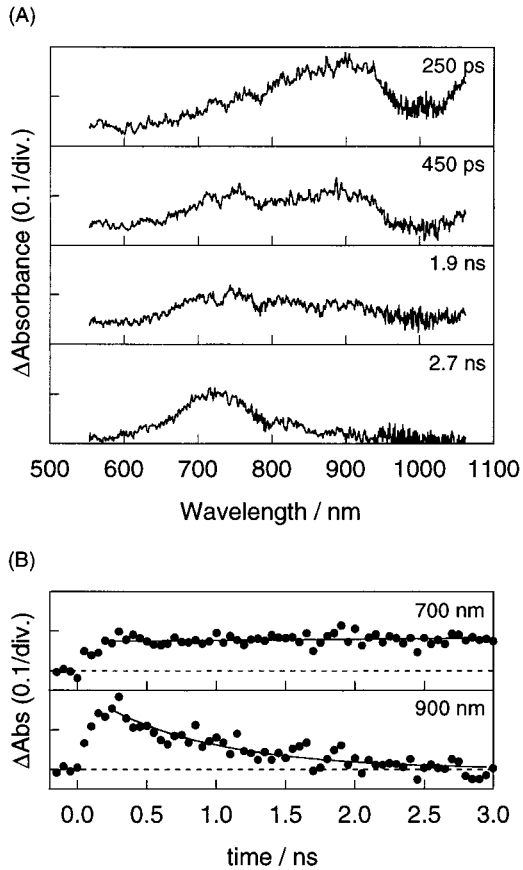

Figure 8. (A) Picosecond transient absorption spectra of BBA−C_{60} in toluene excited with 532 nm laser pulse. (B) Absorption−time profiles at 900 and 700 nm. The solid lines are the fitted curves.

of the rise of BBA−$^3C_{60}$* and the decay of BBA−$^1C_{60}$*. From these findings, it can be concluded that BBA−$^1C_{60}$* deactivated to BBA−$^3C_{60}$* by the intersystem crossing process (eq 3):

$$\text{BBA}-\text{C}_{60} \xrightarrow{h\nu} \text{BBA}-{}^1\text{C}_{60}^* \xrightarrow[isc.]{} \text{BBA}-{}^3\text{C}_{60}^* \qquad (3)$$

Other deactivation pathways of BBA−$^1C_{60}$* can be ruled out in toluene, since the fluorescence decay rate of BBA−C_{60} was the same as that of $C_{61}H_2$.

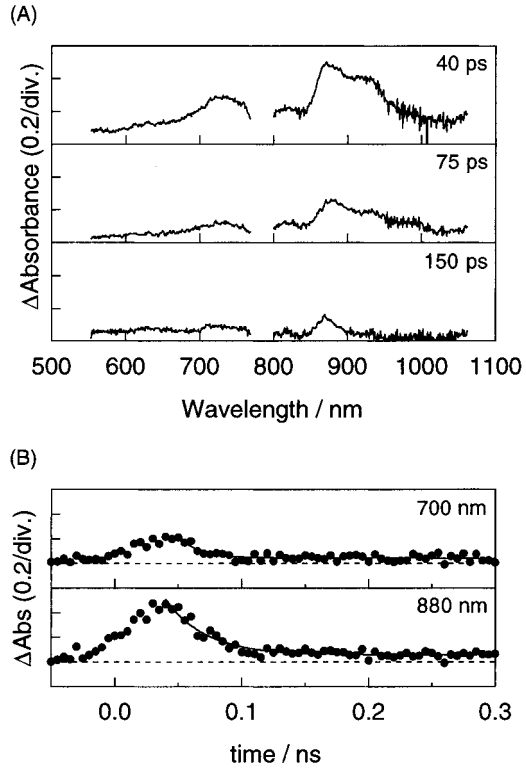

Figure 9. (A) Picosecond transient absorption spectra of BBA−C_{60} in benzonitrile excited with 532 nm laser pulse. (B) Absorption−time profiles. The solid lines are the fitted curves.

Figure 9 A shows spectra of BBA−C_{60} in polar benzonitrile solution. At 40 ps after the laser irradiation, absorption bands were observed at 720 and 880 nm. Both absorption bands can be attributed to the radical cation of BBA moiety from the comparison with the absorption spectrum of $BBA^{\bullet+}$ (Figures 4 and 1S). This finding indicates that CS in BBA−C_{60} is efficient. The absorption band due to the radical anion of C_{60} moiety will be hidden by the intense absorption band of $BBA^{\bullet+}$, as observed in the mixture system of BBA and $C_{61}H_2$ (Figure 4). Since the fluorescence of BBA−$^1C_{60}$* was quenched in benzonitrile as discussed in the previous section, the CS state is considered to be generated from BBA−$^1C_{60}$* as indicated in eq 4:

$$\text{BBA}-\text{C}_{60} \xrightarrow{h\nu} \text{BBA}-{}^1\text{C}_{60}^* \xrightarrow{k_{CS}} \text{BBA}^{\bullet+}-\text{C}_{60}^{\bullet-} \qquad (4)$$

Generation of the CS state was also observed in other polar solvents.

The rate constants for CS from BBA−$^1C_{60}$* (k_{CS}) were estimated from the fluorescence decay rates using eq 5:

$$k_{CS} = 1/\tau_F - 1/\tau_{ref} \qquad (5)$$

where τ_F and τ_{ref} are the fluorescence lifetimes of BBA−C_{60} and that of $C_{61}H_2$ in toluene, respectively. The k_{CS} values in various polar solvents were summarized in Table 1. Furthermore, the quantum yields for CS from BBA−$^1C_{60}$* (Φ_{CS}) were estimated from eq 6:

$$\Phi_{CS} = ((\tau_F)^{-1} - (\tau_{ref})^{-1})/(\tau_F)^{-1} \qquad (6)$$

The k_{CS} and Φ_{CS} values in various solvents are summarized in Table 1. The k_{CS} values tend to increase in polarity of the solvent. In polar solvents, the Φ_{CS} values were almost unity.

TABLE 2: Fluorescence Lifetimes (τ_F) and CS Rates (k_{CS}) of BBA−C_{60} in Anisole at Various Temperatures

T/K	τ_F/s	k_{CS}/s^{-1}
303	4.0×10^{-11}	2.4×10^{10}
298	4.6×10^{-11}	2.1×10^{10}
293	5.0×10^{-11}	1.9×10^{10}
288	5.4×10^{-11}	1.8×10^{10}
283	5.8×10^{-11}	1.7×10^{10}
278	6.5×10^{-11}	1.5×10^{10}
273	7.4×10^{-11}	1.3×10^{10}

Free-energy changes for CS (ΔG_{CS}) from BBA−$^1C_{60}$* were estimated by the method proposed by Weller as listed in Table 1.[20]

To estimate the barrier for the CS step of BBA−C_{60}, the temperature dependence on the k_{CS} rates was investigated. Fluorescence lifetimes and the k_{CS} rates by eq 5 at various temperatures in anisole were estimated as summarized in Table 2. As a reference (τ_{ref}), the fluorescence lifetime of $C_{61}H_2$ was employed, because the fluorescence lifetime of $C_{61}H_2$ did not show temperature dependence within the present temperature range. By employing a modified Arrhenius plot,[3,21] $\ln(k_{CS} \times T^{0.5})$ values showed good linear correlation with $1/T$ as shown in the inset of Figure 7B. From the slope ($= \Delta G^{\#}_{CS}/k_B$, where $\Delta G^{\#}_{CS}$ and k_B are the barrier for the CS step and Boltzman constant, respectively), the $\Delta G^{\#}_{CS}$ value was estimated to be 0.15 eV.

From the classical Marcus equation,[1a,22] $\Delta G^{\#}_{CS}$ has a correlation with ΔG_{CS} as the following equation (eq 7):

$$\Delta G^{\#}_{CS} = (\Delta G_{CS} + \lambda)^2/4\lambda \qquad (7)$$

where λ is the total reorganization energy. The reorganization energy may be partitioned into internal (λ_i) and solvent (λ_s) contributions. Here, $\lambda_i = 0.3$ eV was employed as estimated by Williams et al. based on the charge-transfer absorption and emission maxima of C_{60} and diethylaniline.[3] The solvent reorganization energy was estimated by following equation (eq 8):[1a]

$$\lambda_s = e^2/(4\pi\epsilon_0)[(1/(2r^+) + 1/(2r^-) - 1/R_{cc})(1/n^2 - 1/\epsilon_s)] \qquad (8)$$

where n is refractive index. Employing the geometric parameters summarized in the footnote of Table 1, the λ_s and λ values were evaluated to be 0.3 and 0.6 eV, respectively. From eq 7, the $\Delta G^{\#}_{CS}$ value was evaluated to be 0.10 eV, which is in fairly good agreement with the experimentally estimated value. This good agreement supports the assumption that the λ_i value of the present BBA−C_{60} is similar to that of the dimethylaniline−C_{60} dyad. The good linearity of modified Arrhenius plot (inset of Figure 7B) and the agreement of the $\Delta G^{\#}_{CS}$ value indicate that the CS processes take place in the Marcus "normal region".[21,22] Williams et al. reported that the $\Delta G^{\#}_{CS}$ value of the dimethylaniline−C_{60} dyad connected by three σ-bonds was 0.28 eV in chloroform, which has similar dielectric constant ($\epsilon_s = 4.70$) with anisole ($\epsilon_s = 4.33$).[3] The smaller $\Delta G^{\#}_{CS}$ of BBA−C_{60} will be attributed to smaller total reorganization energy of BBA−C_{60} due to the larger size of BBA than that of dimethylaniline.

Generated radical ions decayed after reaching maximum (Figure 9B). The decay of the absorption bands of the radical ion can be attributed to the CR process. The absorption−time profiles of the radical ions were analyzed by the single-exponential function. The CR rates (k_{CR}^I) were estimated as

TABLE 3: Free-Energy Changes (ΔG_{CR}) and Rates (k_{CR}) for CR in BBA−C_{60} and Lifetimes of Radical Ion Pair (τ_{ion}) in Various Solvents

solvent[a]	$-\Delta G_{CR}^{I}$ eV[b]	k_{CR}^{I} s^{-1}	$-\Delta G_{CR}^{II}$ eV[b]	k_{CR}^{II} s^{-1}	τ_{ion} s
BN	−0.13	2.6×10^{10}	1.37	4.5×10^{6}	2.2×10^{-7}
ANS/BN	−0.07	2.4×10^{10}	1.43	1.6×10^{6}	6.3×10^{-7}
THF	−0.01	3.0×10^{10}	1.49	1.0×10^{6}	1.0×10^{-6}
ANS	0.14	0.2×10^{9}	1.64	1.2×10^{9}	7.1×10^{-10}
ANS/Tol	0.23	2.5×10^{8}	1.73	7.0×10^{8}	1.1×10^{-9}
Tol	0.38		1.88		

[a] Abbreviations for solvents: see footnote of Table 1. [b] $-\Delta G_{CR}^{I} = (-\Delta G_{CR}^{II}) - {}^3E_{00}$, $-\Delta G_{CR}^{II} = E_{ox}(D) - E_{red}(A) + \Delta G_S$, where ${}^3E_{00}$ is the triplet energy of the fullerene moiety (${}^3E_{00} = 1.50$ eV).

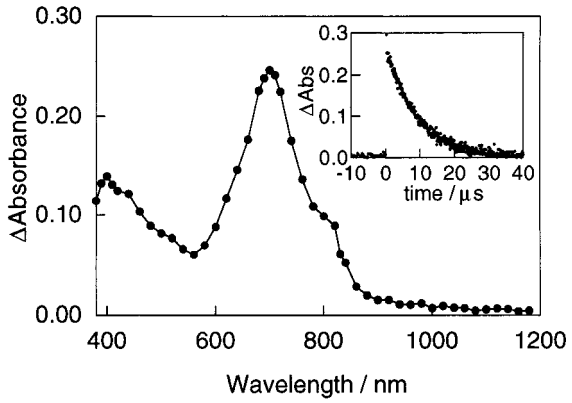

Figure 10. Nanosecond transient absorption spectrum of BBA−C_{60} in toluene at 250 ns after 532 nm laser excitation. Inset: Absorption−time profile at 700 nm.

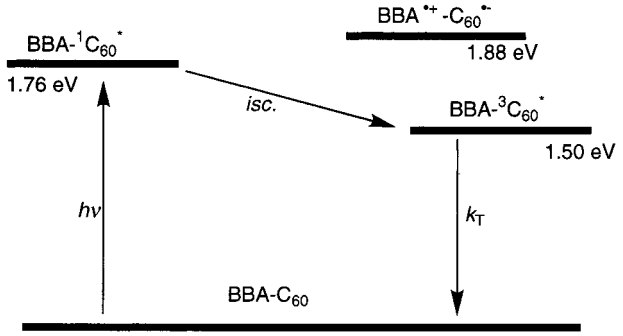

Figure 11. Schematic energy diagram for photoprocesses of BBA−C_{60} in toluene.

summarized in Table 3. The CR rates tend to increase in polar solvents, suggesting the CR process is in the Marcus "inverted region".

Nanosecond Transient Absorption Spectra of the BBA−C_{60} Dyad. The photoinduced processes of BBA−C_{60} in a longer time region were investigated by the nanosecond laser photolysis. Upon excitation of BBA−C_{60} in toluene with the 532 nm laser pulse, a transient absorption band appeared at 710 nm of which the lifetime was 4.2 μs (Figure 10). The transient absorption band can be assigned to BBA−$^3C_{60}$* by comparison with the absorption spectrum of $^3C_{61}H_2$* (Figure 3). In toluene, therefore, the photoinduced CS process was not observed both in the singlet and triplet excited states. The poor reactivity of BBA−C_{60} in toluene can be attributed to a thermodynamically unstable CS state. On the basis of the free-energy changes (Table 1), the energy diagram was constructed as shown in Figure 11. In toluene, the energy level of the CS state is located at higher energy than that of BBA−$^1C_{60}$* by 0.12 eV, indicating that CS in toluene is a thermodynamically inaccessible state.

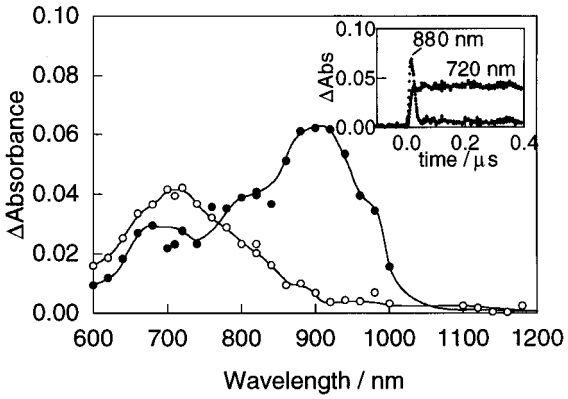

Figure 12. Nanosecond transient absorption spectra of BBA−C_{60} in anisole at 25 ns (closed circle) and 250 ns (open circle) after 532 nm laser excitation. Inset: Absorption−time profiles at 880 and 720 nm.

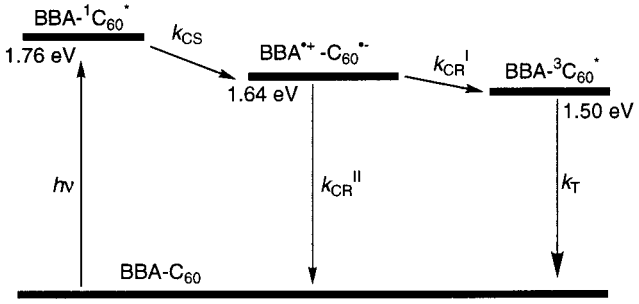

Figure 13. Schematic energy diagram for photoprocesses of BBA−C_{60} in anisole.

In the case of BBA−C_{60} in anisole, the absorption band at 880 nm decayed fast, while the absorption band at 720 nm had a long lifetime (Figure 12). The absorption bands at 880 and 720 nm correspond to BBA$^{•+}$−$C_{60}^{•-}$ and BBA−$^3C_{60}$*, respectively. BBA−$^3C_{60}$* is considered to be formed by CR of BBA$^{•+}$−$C_{60}^{•-}$, because almost BBA−$^1C_{60}$* undergoes to CS ($\Phi_{CS} = 0.95$ in anisole). Triplet state formations via CR was also observed in anisole/toluene mixture solvent. The CR processes which generate triplet states have been reported for other dyad molecules.[5−7] The absorption intensity of BBA−$^3C_{60}$* in anisole is ca. 1/6 of that in toluene under the same photolysis condition, indicating that ca. 5/6 of BBA$^{•+}$−$C_{60}^{•-}$ recombined to form BBA−C_{60} in the ground state as indicated in the schematic energy diagram (Figure 13). Therefore, the CR rates generating BBA−$^3C_{60}$* and BBA−C_{60} (k_{CR}^{I} and k_{CR}^{II}, respectively) were estimated to be 0.2×10^9 and 1.2×10^9 s^{-1}, respectively. As for CR in anisole/toluene mixture, the k_{CR}^{I} and k_{CR}^{II} values were estimated as listed in Table 3. The triplet formation from BBA$^{•+}$−$C_{60}^{•-}$ in anisole and anisole/toluene can be attributed to the relatively high energy level of the CS state from which BBA−$^3C_{60}$* is also accessible as indicated in Figure 13. Free-energy changes for the generation of BBA−$^3C_{60}$* and the ground state via the CS state (ΔG_{CR}^{I} and ΔG_{CR}^{II}, respectively) were also summarized in Table 3.

By excitation of BBA−C_{60} in benzonitrile with the 532 nm laser pulse, transient absorption bands appeared at 700 and 880 nm (Figure 14). These absorption bands can be attributed to the radical cation of the BBA moiety, indicating that BBA$^{•+}$−$C_{60}^{•-}$ is persistent in the submicrosecond region. Therefore, in benzonitrile, BBA$^{•+}$−$C_{60}^{•-}$ decayed by two steps: One is decay within 1 ns, and the another is decay in the submicrosecond region. The decay rate constant of BBA$^{•+}$−$C_{60}^{•-}$ (k_{CR}^{II}) was estimated to be 4.5×10^6 s^{-1}, which corresponds to 220 ns of the ion pair lifetime (τ_{ion}). It should be noted that the CS state

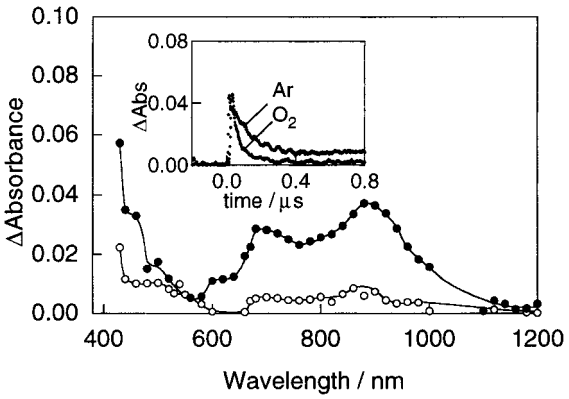

Figure 14. Nanosecond transient absorption spectra of BBA−C_{60} in benzonitrile at 100 ns (closed circle) and 1 μs (open circle) after 532 nm−laser excitation. Inset: Absorption−time profiles at 880 nm in argon- and oxygen-saturated solutions.

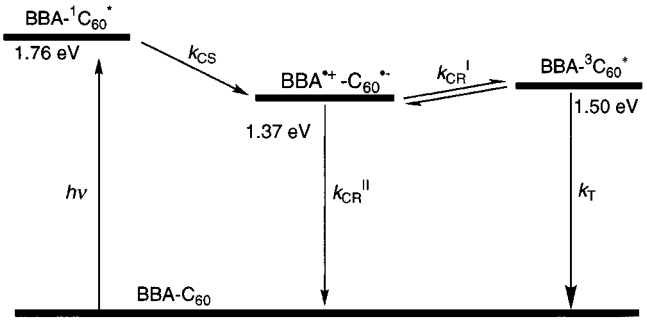

Figure 15. Schematic energy diagram for photoprocesses of BBA−C_{60} in benzonitrile.

with lifetime in the submicrosecond region is quite a rare case. Usually, the CS states recombine within a few nanoseconds in many donor−acceptor dyad systems. Similar long-lived CS state was also observed in tetrahydrofuran and anisole/benzonitrile mixture (Table 3). In tetrahydrofuran, τ_{ion} was estimated to be 1.0 μs.

In the spectrum of Figure 14, the ratio of signal intensity at 700 nm to that of 880 nm is somewhat larger than that of radical cation of BBA (Figures 4 and 1S), indicating that the triplet state (BBA−$^3C_{60}$*) is also included in the absorption band around 700 nm. The absorption bands due to BBA$^{\bullet+}$−$C_{60}^{\bullet-}$ as well as that of BBA−$^3C_{60}$* were quenched in the presence of oxygen as indicated in the inset of Figure 14. In the previous section, it was shown that the radical cation of BBA is oxygen-insensitive. Therefore, the following possibilities can be expected for the CS state in the submicrosecond region: (A) BBA$^{\bullet+}$−$C_{60}^{\bullet-}$ in the submicrosecond region is generated via BBA−$^3C_{60}$*. (B) BBA$^{\bullet+}$−$C_{60}^{\bullet-}$ in the submicrosecond region is in an equilibrium with BBA−$^3C_{60}$* (Figure 15). Because of extensive spectral overlap of BBA$^{\bullet+}$−$C_{60}^{\bullet-}$ and BBA−$^3C_{60}$* (Figure 14), we cannot exclude one of the two possibilities by kinetic analyses. In the present case, intermolecular electron-transfer process, i.e., electron transfer between BBA−$^3C_{60}$* and BBA−C_{60}, can be ruled out, since the absorption−time profile of BBA$^{\bullet+}$−$C_{60}^{\bullet-}$ did not show dependence on the concentration and laser power. It should be stressed that most part of BBA$^{\bullet+}$−$C_{60}^{\bullet-}$ decreased within 100 ps as shown in the absorption−time profile of Figure 9B. Therefore, the long-lived CS state is a minor component (ca. 10%).

Transient absorption spectra of BBA−C_{60} in benzonitrile were estimated at several temperatures (See Supporting Information, Figure 2S). It was revealed that the ratio of the absorbance at 700 nm to that at 880 nm decreased as the temperature became low; 0.94 at 303 K, while 0.68 at 273 K. As indicated in the previous section, the absorption band at 700 nm includes contribution of BBA−$^3C_{60}$*. These findings support the consideration that the CS state and triplet state are in the equilibrium in which generation of the triplet state from CS state is endothermic as shown in the energetic diagram (Figure 15). It should be noted that such behavior including the equilibria between CS state and triplet state has been reported for some other intramolecular systems,[7b,c,23] in which the CS state shows the lifetime of microsecond region. These results indicate that the relative energy level of the excited triplet state to the CS state is a quite important parameter to optimize the lifetime of the CS state of the dyad molecules.

Conclusions

The CS of the BBA−C_{60} dyad proceeded quite effectively in the polar solvents, although the CS was not observed in nonpolar toluene. The CS rates were on the order of 10^{10} s^{-1} and the quantum yields were almost unity. The CS process in these solvents can be explained on the basis of the free-energy changes. As for the CR processes, two types of the deactivation were observed. In moderately polar solvent (i.e., anisole), the CS state recombined to form the ground state and the excited triplet state (BBA−$^3C_{60}$*), while the formation of the triplet state was a minor process. On the other hand, in polar solvents ($\epsilon_s > 7$), the CS state was deactivated by two steps. Most of the CS state deactivated to the ground state, while the minor part shows the lifetime of the submicrosecond region. The long-lived charge separated state is considered to be in an equilibrium with the excited triplet state and/or generated from the triplet excited state. These findings indicate that the relative energy level of the excited triplet state to the CS state is a quite important parameter to optimize the lifetime of the CS state of the dyad molecules aiming at the light-energy conversion system.

Acknowledgment. The present work was partly supported by a Grant-in-Aid on Scientific Research from the Ministry of Education, Science, Sports and Culture of Japan (No. 10207202, 11740380, and 12875163). The authors are also grateful for financial support by Core Research for Evolutional Science and Technology (CREST) of Japan Science and Technology Corporation.

Supporting Information Available: Absorption spectrum of radical cation of BBA and transient absorption spectra of BBA−C_{60} in benzonitrile at 303 and 273 K. This material is available free of charge via the Internet at http://pubs.acs.org.

References and Notes

(1) For reviews, see: (a) Wasielewski, M. R. *Chem. Rev.* **1992**, *92*, 435. (b) Gust, D.; Moore, T. A.; Moore, A. L. *Acc. Chem. Rec.* **1993**, *26*, 198. (c) Paddon-Row, M. N. *Acc. Chem. Rec.* **1994**, *27*, 18.

(2) For a review, see: Martin, N.; Sánchez, I.; Illescas, B.; Pérez, I. *Chem. Rev.* **1998**, *98*, 2527.

(3) (a) Williams, R. M.; Zwier, J. M.; Verhoeven, J. W. *J. Am. Chem. Soc.* **1995**, *117*, 4093. (b) Williams, R. M.; Koeberg, M.; Lawson, J. M.; An, Y.-Z.; Rubin, Y.; Paddon-Row, M. N.; Verhoeven, J. W. *J. Org. Chem.* **1996**, *61*, 5055.

(4) Imahori, H.; Cardoso, S.; Tatman, D.; Lin, S.; Noss, L.; Seely, G. R.; Sereno, L.; Silber, C.; Moore, T. A.; Moore, A. L.; Gust, D. *Photochem. Photobiol.* **1995**, *62*, 1009.

(5) (a) Kuciauskas, D.; Lin, S.; Seely, G. R.; Moore, A. L.; Moore, T. A.; Gust, D.; Drovetskaya, T.; Reed, C. A.; Boyd, P. D. W. *J. Phys. Chem.* **1996**, *100*, 15926. (b) Imahori, H.; Hagiwara, K.; Aoki, M.; Akiyama, T.; Taniguchi, S.; Okada, T.; Shirakawa, M.; Sakata, Y. *J. Am. Chem. Soc.* **1996**, *118*, 11771. (c) Imahori, H.; Hagiwara, K.; Akiyama, T.; Aoki, M.; Taniguchi, S.; Okada, T.; Shirakawa, M.; Sakata, Y. *Chem. Phys. Lett.* **1996**,

263, 545. (d) Imahori, H.; Ozawa, S.; Uchida, K.; Takahashi, M.; Azuma, T.; Ajavakom, A.; Akiyama, T.; Hasegawa, M.; Taniguchi, S.; Okada, T.; Sakata, Y. *Bull. Chem. Soc. Jpn.* **1999**, *72*, 485. (e) Tkachenko, N. V.; Rantala, L.; Tauber, A. Y.; Helaja, J.; Hynninen, P. V.; Lemmetyinen, H. *J. Am. Chem. Soc.* **1999**, *121*, 9378. (f) Schuster, D. I.; Cheng, P.; Wilson, S. R.; Prokhorenko, V.; Katterle, M.; Holzwarth, A. R.; Braslavsky, S. E.; Klihm, G.; Williams, R. M.; Luo, C. *J. Am. Chem. Soc.* **1999**, *121*, 11599.

(6) (a) Llacay, J.; Veciana, J.; Vidal-Gancedo, J.; Bourdelnde, J. L.; González-Moreno, R.; Rovira, C. *J. Org. Chem.* **1998**, *63*, 5201. (b) Martin, N.; Sánchez, L.; Herranz, M. A.; Guldi, D. M. *J. Phys. Chem. A* **2000**, *104*, 4648.

(7) (a) Yamashiro, T.; Aso, Y.; Otsubo, T.; Tang, H.; Harima, T.; Yamashita, K. *Chem. Lett.* **1999**, 443. (b) Fujitsuka, M.; Ito, O.; Yamashiro, T.; Aso, Y.; Otsubo, T. *J. Phys. Chem. A* **2000**, *104*, 4876. (c) Fujitsuka, M.; Matsumoto, K.; Ito, O.; Yamashiro, T.; Aso, Y.; Otsubo, T. *Res. Chem. Intermed.*, in press. (d) Hirayama, D.; Yamashiro, T.; Takimiya, K.; Aso, Y.; Otsubo, T.; Norieda, H.; Imahori, H.; Sakata, Y. *Chem. Lett.* **2000**, 570.

(8) (a) Sariciftci, N. S.; Wudl, F.; Heeger, A. J.; Maggini, M.; Scorrano, G.; Prato, M.; Bourassa, J.; Ford, P. C. *Chem. Phys. Lett.* **1995**, *247*, 510. (b) Maggini, M.; Guldi, D. M.; Mondini, S.; Scorrano, G.; Paolucci, F.; Ceroni, P.; Roffia, S. *Chem. Euro. J.* **1998**, *4*, 1992. (c) Polese, A.; Mondini, S.; Bianco, A.; Toniolo, C.; Scorrano, G.; Guldi, D. M.; Maggini, M. *J. Am. Chem. Soc.* **1999**, *121*, 3446. (d) Guldi, D. M.; Maggini, M.; Scorrano, G.; Prato, M. *J. Am. Chem. Soc.* **1997**, *119*, 974. (e) Guldi, D. M.; Garscia, G. T.; Mattay, J. *J. Phys. Chem. A* **1998**, *102*, 9679. (f) Guldi, D. M. *Chem. Commun.* **2000**, 321.

(9) Kuwabara, Y.; Ogawa, H.; Inada, H.; Noma, N.; Shirota, Y. *Adv. Mater*. **1994**, *6*, 677.

(10) (a) Guldi, D. M.; Hungerbühler, H.; Asmus, K.-D. *J. Phys. Chem.* **1995**, *99*, 9380. (b) Guldi, D. M.; Asmus, K.-D. *J. Phys. Chem. A* **1997**, *101*, 1472. (c) Guldi, D. M.; Hungerbühler, H.; Asmus, K.-D. *J. Phys. Chem. A* **1997**, *101*, 1783. (d) Guldi, D. M. *J. Phys. Chem. A* **1997**, *101*, 3895. (e) Riggs, J. E.; Sun, Y.-P. *J. Phys. Chem. A* **1999**, *103*, 485. (f) Sun, Y.-P.; Guduru, R.; Lawson, G. E.; Mullins, J. E.; Guo, Z.; Quinlan, J.; Bunker, C. E.; Gord, J. R. *J. Phys. Chem. B* **2000**, *104*, 4625. (g) Prat, F.; Stackow, R.; Bernstein, R.; Qian, W.; Rubin, Y.; Foote, C. S. *J. Phys. Chem. A* **1999**, *103*, 7230. (h) Bensasson, R. V.; Bienvenue, E.; Fabre, C.; Janot, J. M.; Land, E. J.; Leach, S.; Leboulaire, V.; Rassat, A.; Roux, S.; Seta, P. *Chem. A, Euro. J.* **1998**, *4*, 270. (i) Pasimeni, L.; Hirsch, A.; Lamparth, I.; Herzog, A.; Maggini, M.; Prato, M.; Corvaja, C.; Scorrano, G. *J. Am. Chem. Soc.* **1997**, *119*, 12896. (j) Pasimeni, L.; Hirsch, A.; Lamparth, I.; Maggini, M.; Prato, M. *J. Am. Chem. Soc.* **1997**, *119*, 12902. (k) Hetzer, M.; Gutberlet, T.; Brown M. F.; Camps, X.; Vostrowsky, O.; Schonberger, H.; Hirsch, A.; Bayerl, T. M. *J. Phys. Chem. A* **1999**, *103*, 637.

(11) Ohno, T.; Moriwaki, K.; Miyata, T. Submittd for publication.

(12) Kim, D.; Lee, M.; Suh, Y. D.; Kim, S. K. *J. Am. Chem. Soc.* **1992**, *114*, 4429.

(13) Ma, B.; Sun, Y.-P. *J. Chem. Soc., Perkin Trans. 2* **1996**, 2157.

(14) Biczok, L.; Linschitz, H.; Walter, R. I. *Chem. Phys. Lett.* **1992**, *195*, 339.

(15) Fujitsuka, M.; Luo, C.; Ito, O. *J. Phys. Chem. B* **1999**, *103*, 445.

(16) Rehm, D.; Weller, A. *Isr. J. Chem.* **1970**, *8*, 259.

(17) Murov, S. L.; Carmichael, I.; Hug, G. L. *Handbook of Photochemistry*, 2nd ed.; Marcel Dekker: New York, 1993.

(18) Konishi, T.; Fujitsuka, M.; Ito, O. *Chem. Lett.* **2000**, 202.

(19) The ϵ_C value was estimated by the chemical oxidation by $FeCl_3$.

(20) Weller, A. *Z. Phys. Chem., Neue Folge.* **1982**, *133*, 93.

(21) (a) Zeng, Y.; Zimmt, M. B. *J. Phys. Chem.* **1992**, *96*, 8395. (b) Kroon, J.; Oevering, H.; Verhoeven, J. W.; Warman, J. M.; Oliver, A. M.; Paddon-Row, M. N. *J. Phys. Chem.* **1993**, *97*, 5065.

(22) Marcus, R. A. *J. Chem. Phys.* **1956**, *24*, 966.

(23) (a) van Dijk, S. I.; Groen, C. P.; Hartl, F.; Brouwer, A. M.; Verhoeven, J. W. *J. Am. Chem. Soc.* **1996**, *118*, 8425. (b) Smit, K. J.; Warman, J. M. *J. Lumin.* **1988**, *42*, 149. (c) Anglos, D.; Bindra, V.; Kuki, A. *J. Chem. Soc., Chem. Commun.* **1994**, 213.